Plasmonics
DOI 10.1007/s11468-011-9313-5

Plasmon Singularities from Metal Nanoparticles in Active Media: Influence of Particle Shape on the Gain Threshold

Min Cao · Meng Wang · Ning Gu

Received: 22 August 2011 / Accepted: 21 November 2011

Abstract Localized surface plasmon singularities from metal nanoparticles in active media are investigated on the basis of classic linear electrodynamics. It is found that the gain threshold is inversely proportional to the shape factor of the particle. When relating this phenomenon to the plasmonic field-enhanced emission from gain units, we show that the maximum electric field around spheroidal particles impacts upon the gain threshold via a two-exponential decay function. Our results provide a way to reduce the gain requirement in metal nanoparticle-based spaser or random laser systems.

Keywords Plasmon singularity · Metal nanoparticles · Gain threshold

Introduction

Over the past decades, nobel metal nanoparticles have attracted significant attention due to their unique localized surface plasmon resonance (LSPR) properties, which originate from the collective oscillation of conduction electrons in response to optical excitation. The resonance creates enhanced light scattering and absorption and large local field enhancement, strongly depending on the shape, composition, and arrangement of the particles, and the properties of local environment. By changing these factors, one can control the design of desired metamaterials for applications in sensing [1, 2], imaging [3, 4], and medical diagnostic [5].

Recent studies have shown that incorporation of optical gain into the adjacent dielectric can compensate absorption in metal and thus enable new applications of metamaterials [6–8]. Of particular interest are single metal nanospheres in a medium with threshold gain that exhibit a plasmon singularity, which theoretically results in an infinite local field and scattering cross section [9]. A relevant phenomenon of surface plasmon amplification by stimulated emission of radiation (spaser) [10], based on Förster energy transfer from excited molecules to resonating metallic nanostructures, was recently experimentally demonstrated [11]. And random lasing resonance was observed and controlled by incorporating metallic nanoparticles into optical gain media [12, 13]. Strong coupling occurring between metallic nanoparticles and gain medium was reported in gain-assisted and gain-functionalized systems [14]. Meanwhile, theoretical analysis of the spaser phenomena was carried out on metallic nanoparticles with different geometries [15–18]. However, the influence of particle shape on the threshold value of the lasing gain in the surrounding medium has not yet been reported.

In this letter, using electrodynamics calculations of the plasmon singularity, we investigate the dependence of the gain threshold on the shape of metal nanoparticles, with the aim to give a conceptual understanding for the nature of gain requirement in gain-assisted metal nanoparticle systems.

M. Cao · M. Wang · N. Gu (✉)
State Key Laboratory of Bioelectronics and Jiangsu Laboratory for Biomaterials and Devices,
Southeast University, Nanjing 210096, China
e-mail: guning@seu.edu.cn

M. Cao
School of Science, Nantong University, Nantong 226007, China

Published online: 13 December 2011

Electrodynamic Methods

The LSPR spectra of metal nanoparticles can be calculated by solving Maxwell's equations under appropriate boundary conditions. In the limit of very small particles, a quasi-static approximation greatly simplifies the problem and leads to an intuitive understanding of the optical response in terms of dipolar radiation [19]. For an isolated metal nanoparticle in the quasi-static limit (particle size less than ∼ 50 nm), the Clausius–Mossotti dipole polarizability takes the form [20]:

$$\alpha = V\varepsilon_m (1+\kappa)\left(\frac{\varepsilon-\varepsilon_m}{\varepsilon+\kappa\varepsilon_m}\right) \quad (1)$$

where V is the particle volume, ε and ε_m are permittivities of the particle and surrounding medium, respectively, and κ is the shape factor, e.g., $\kappa = 2$ for spheres. The far-field scattering cross section is obtained from the polarizability using the optical theorem [21]:

$$\sigma_{sca} = \frac{8\pi^3}{3\lambda^4}|\alpha|^2 \quad (2)$$

On the basis of classic linear electrodynamics, the gain medium is considered as a dielectric with a negative imaginary part, i.e., $\varepsilon_m = \varepsilon'_m + i\varepsilon''_m$, where ε'_m is the real part of the dielectric response commonly used to determine the resonance wavelength and ε''_m is the imaginary part that represents the amplifying response of the medium. For noble metals like Ag and Au, ε can be well approximated by the modified Drude model [22, 23]:

$$\varepsilon(\omega) = \varepsilon_b - \frac{\omega_p^2}{\omega^2 + i\omega\gamma} \quad (3)$$

where ε_b is the contribution from bound electrons in the metal, ω_p is the bulk plasma frequency that is related to the density of conduction electrons, and γ is the damping constant for the electrons. Separating Eq. 3 into real and imaginary components and noting that at optical frequencies $\omega \gg \gamma$ give

$$\varepsilon' = \varepsilon_b - \frac{\omega_p^2}{\omega^2} \quad (4)$$

and

$$\varepsilon'' = \frac{\gamma\omega_p^2}{\omega^3} \quad (5)$$

From Eq. 1, the plasmon resonance occurs whenever the condition of $\varepsilon' = -\kappa\varepsilon'_m$ is fulfilled. This leads to the LSPR wavelength given by

$$\lambda_0 = \frac{2\pi c}{\omega_p}\left(\varepsilon_b + \kappa\varepsilon'_m\right)^{1/2} \quad (6)$$

where c is the speed of light. At the wavelength, if the imaginary part in the denominator of Eq. 1 becomes zero, then plasmon singularity occurs along with extremely large scattering cross section (see Eq. 2). This condition can be satisfied with

$$\varepsilon''_m = -\frac{\gamma}{\kappa\omega_p}\left(\varepsilon_b + \kappa\varepsilon'_m\right)^{3/2} \quad (7)$$

The gain threshold is therefore obtained as follows [7, 9, 24]:

$$g_{th} = -\frac{2\pi}{\lambda_0}\frac{\varepsilon''_m}{\sqrt{\varepsilon'_m}} = \frac{\gamma}{c}\left(\frac{\varepsilon_b}{\kappa\sqrt{\varepsilon'_m}} + \sqrt{\varepsilon'_m}\right) \quad (8)$$

Here, the gain medium under consideration is composed of optically pumped dye molecules or semiconductor nanoparticles (as gain units) dispersed in solution. The gain coefficient g is related to the stimulated emission cross section σ_e and the density N via $g = N\sigma_e$ [24, 25]. The resonator (or cavity) that supports surface plasmon modes can be any metal nanoparticles, but a good overlap of the resonant response with the emission spectrum of gain units should be ensured [18]. In this letter, we consider prolate ellipsoid nanoparticles with the polarization along the major axes, the shape factor

$$\kappa = \frac{1-L}{L} \quad (9)$$

with depolarization factor L given by

$$L = \frac{abd}{2}\int_0^\infty \frac{dq}{(a^2+q)\sqrt{(a^2+q)(b^2+q)(d^2+q)}} \quad (10)$$

where a, b, and d are the semiaxes.

In the following calculations, the Drude parameters are assigned as $\varepsilon_b = 9.5$, $\hbar\omega_p = 8.95$ eV, and $\hbar\gamma = 0.067$ eV for gold [26, 27], while $\varepsilon_b = 3.9$, $\hbar\omega_p = 9.2$ eV, and $\hbar\gamma = 0.021$ eV for silver [28, 29].

Results and Discussion

Figure 1a, b shows the dependence of gain threshold g_{th} and imaginary part ε''_m on the aspect ratio of gold and silver nanospheroids, respectively. The real part ε'_m is set equal to 1.77 (aqueous). It can be seen that, with increasing the aspect ratio from 1.0 to 8.0, the value of ε''_m first increases and then decreases, while the gain threshold g_{th} decreases all along. In fact, as indicated in Eq. 8, the gain threshold is inversely proportional to the shape factor κ, which rises exponentially with increasing particle aspect ratio. This means that one

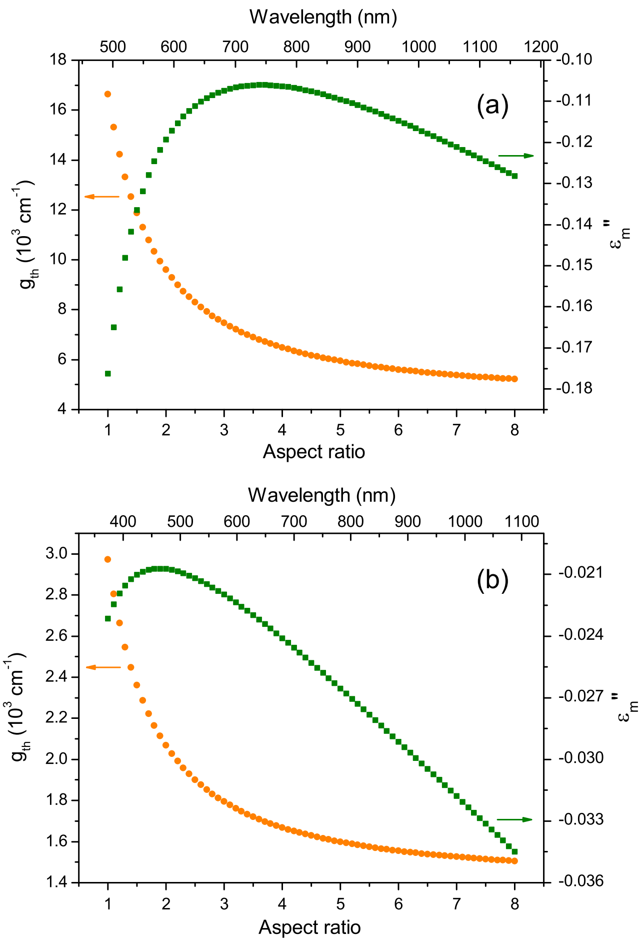

Fig. 1 Calculated gain threshold g_{th} and imaginary part ε''_m plotted against the aspect ratio of **a** gold and **b** silver prolate nanospheroids with $\varepsilon'_m = 1.77$. The corresponding LSPR wavelength is shown on the *top axis*

can lower the gain threshold by optimizing the particle shape. There is about 3-fold decrease of gain threshold for gold prolate spheroids with high aspect ratio compared to that for gold spheres, as seen in Fig. 1a. For silver spheroids with aspect ratio of 5.0–8.0, the value of g_{th} is $\sim 1.6 \times 10^3\text{cm}^{-1}$ (see Fig. 1b) that is quite possible to achieve experimentally [13]. Using a typical value of $\sigma_e = 2.5 \times 10^{-16}\text{cm}^2$ [9], one can estimate the threshold number of excited dye molecules per nanoparticle to be $\sim 2.9 \times 10^2$, when taken per volume occupied by a silver spheroid particle with an equivalent volume to a 22-nm radius sphere. This number is far less than that is required to realize a spaser experimentally [11]. In addition, spheroid particles have a plasmon mode with stable polarization along the major axis [18], making them excellent candidates for the spaser.

Note here the onset of electronic interband transitions from the valence band to the Fermi level causes a sharp increase in the imaginary part ε'', which is not included in Eq. 3. Consequently, for the resonance energy close to the edge of interband transitions region (ca. 2.5 eV for gold and 3.8 eV for silver) [30], more gain is required to compensate Joule losses caused by interband damping. As for particles we considered, their LSPR energy are mostly beyond the edge (see Fig. 1). So it does not affect the trend in the dependence of gain threshold on the shape factor.

The underlying physics of the behavior in gain units adjacent to the metal nanoparticle is believed to be closely associated with the plasmonic field [8, 13, 31]. Therefore, the influence of local electric field on the gain threshold is investigated. The fields around metal nanoparticles are known to be varied with the polar angle of the target. For simplicity, we consider the maximum local field on the particle surface, which can be expressed as follows [32]:

$$E_{\max} = \sqrt{|1-\beta|^2 + \frac{2\text{Re}\,((1-\beta)\,\beta^*)}{L} + \frac{|\beta|^2}{L^2}}\, E_0 \approx \kappa|\beta|\, E_0 \tag{11}$$

where E_0 is the incident electric field and $\beta = (\varepsilon - \varepsilon_m)/(\varepsilon + \kappa\varepsilon_m)$, which has an absolute value of about $(1+\kappa)\,\varepsilon'_m\omega_p/\gamma\,(\varepsilon_b + \kappa\varepsilon'_m)^{3/2}$ at the resonant frequency. The maximum local field is seen to be dependent on the shape and composition of the particle and on the dielectric properties of the medium. Consider the effect of the shape alone, the maximum field $E_{\max}$ is found to increase monotonously with increasing the shape factor κ for each metal and fixed value of ε'_m (see, for example, the inset in Fig. 2b). The opposite tendency between $g_{th} - \kappa$ and $E_{\max} - \kappa$ suggests an intriguing relationship between g_{th} and $E_{\max}$. Combining Eqs. 8 and 11 to eliminate the shape factor κ, one gets a complex relation between g_{th} and $E_{\max}$. However, Fig. 2 shows that g_{th} decreases continuously with increasing $E_{\max}/E_0$ for each metal and fixed value of ε'_m. Furthermore, all these curves can be accurately described by the sum of two exponents, resulting in $g_{th} \propto a_1\exp(-E_{\max}/\tau_1) + a_2\exp(-E_{\max}/\tau_2)$, where a_1, a_2, τ_1, and τ_2 are coefficients. That is, as the local electric field of the metal nanoparticles is increased, the gain threshold decreases at first sharply and then gently. This can be understood since the high local fields created by the LSPR can excite the gain units and stimulate more emission and then lower the gain threshold. Additionally, excited gain units can undergo near-field interactions with metals, amplifying plasmons that are then radiated into free space. This interaction process yields the very strong feedback in the spaser [18], until limited by saturation effects [9]. So the shape dependence of

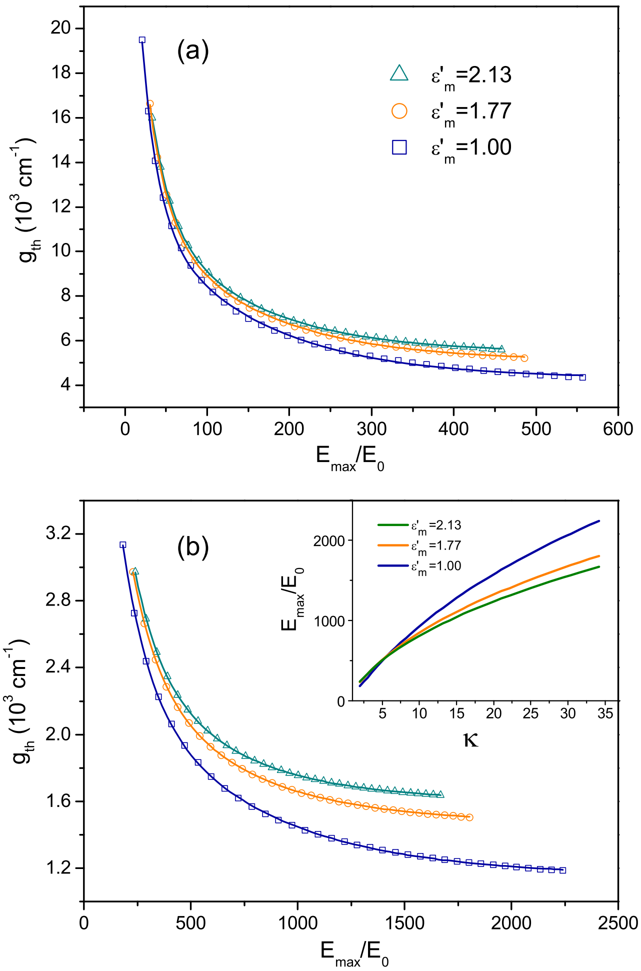

Fig. 2 Calculated gain threshold g_{th} plotted against the maximum normalized field $E_{\max}/E_0$ of **a** gold and **b** silver prolate nanospheroids with various aspect ratio for different values of ε'_m. The particle aspect ratio varies from 1.0 to 8.0 with a step of 0.2. The *solid lines* are fits of the data to the two-exponential decay function. The *inset* in **b** shows a plot of the maximum normalized field $E_{\max}/E_0$ as a function of the shape factor κ of silver prolate nanospheroids for different values of $\varepsilon'_{\mathrm{m}}$

the gain threshold can be explained with the plasmonic field-controlled gain availability in the systems. It is also noticed that the maximum local field $E_{\max}$ decreases with an increase in $\varepsilon'_{\mathrm{m}}$ for high values of κ, which consequently results in the increase of g_{th}.

Now we estimate the local electric field at the singularity when saturation effects from the gain medium are taken into account. Following the spirit and notation of [9], we express Δ (the ratio of the maximum local field $E_{\max}$ to the saturation electric field E_{s}) in a self-consistent equation:

$$\Delta^3 + (1+\eta_2)\,\Delta = \kappa\eta_1\Delta_0\left(1+\Delta^2\right) \tag{12}$$

where $\Delta_0 = E_0/E_{\mathrm{s}}$, $\eta_1 = (1+\kappa)\,\varepsilon'_{\mathrm{m}}/\varepsilon''$, and $\eta_2 = \kappa\varepsilon''_{\mathrm{m}}/\varepsilon''$. Numerical results of the maximum plasmonic field in the active medium are summarized in Fig. 3, where Δ is plotted against η_2 for silver prolate nanospheroids with various shape factor κ. The incident field value Δ_0 is set to 10^{-10} and $\varepsilon'_{\mathrm{m}}$ is set to 1.77. It can be seen that, when the gain medium has a high saturation intensity and a gain coefficient exceeding the threshold ($\eta_2 < -1$), the value of the plasmonic field ultimately reaches a steady-state value near E_{s}, which is independent of the shape factor κ. And in the saturable-absorption case ($\eta_2 > 0$), Δ remains close to $\kappa\eta_1\Delta_0$ which increases with increasing κ for a fixed $\varepsilon'_{\mathrm{m}}$.

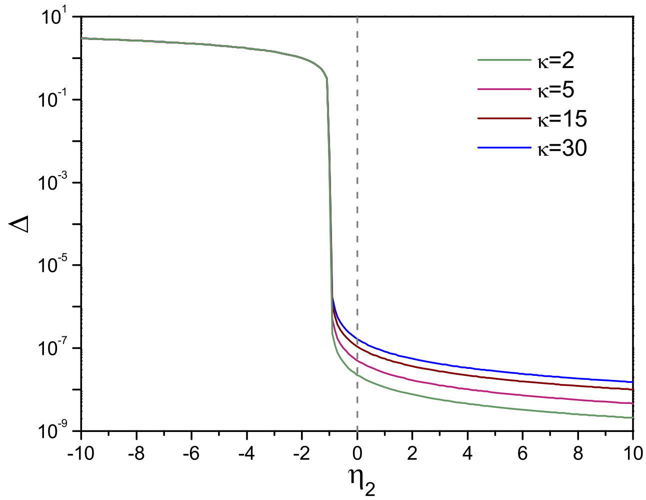

Fig. 3 The maximum local field (given in units of E_{s}) plotted against η_2 for silver prolate nanospheroids with various shape factor κ when $\Delta_0 = 10^{-10}$ and $\varepsilon'_{\mathrm{m}} = 1.77$

Conclusions

In conclusion, we have studied the condition for the plasmon singularity in gain-assisted metal nanoparticle systems. It is interesting to find that the gain threshold has a reciprocal relationship with the shape factor of the particle. When relating the shape factor to the local plasmonic field, we showed that the maximum electric field around the spheroid particle impacts upon the gain threshold via a two-exponential decay function. We also showed that when the active medium has a gain exceeding the threshold, the local electric field at the singularity evolves to a steady-state value near E_{s} due to the saturation effects, which is independent of the shape factor. Our results provide a conceptual understanding for the nature of gain requirement in metal nanoparticle-based spaser or random laser systems.

Acknowledgements This work is supported by grants from the National Basic Research Program of China (no. 2011CB933500), National Natural Science Foundation of China (nos. 60725101, 50872021, and 30970754), and China international S & T cooperation project (no. 2009DFA31990).

References

1. Mayer KM, Hafner JH (2011) Localized surface plasmon resonance sensors. Chem Rev 111:3828–3857
2. Fang ZY, Cai JY, Yan ZB, Nordlander P, Halas NJ, Zhu X (2011) Removing a wedge from a metallic nanodisk reveals a Fano resonance. Nano Lett 11:4475–4479
3. Yong KT, Swihart MT, Ding H, Prasad PN (2009) Preparation of gold nanoparticles and their applications in anisotropic nanoparticle synthesis and bioimaging. Plasmonics 4:79–93
4. Fang ZY, Peng Q, Song WT, Hao FH, Wang J, Nordlander P, Zhu X (2011) Plasmonic focusing in symmetry broken nanocorrals. Nano Lett 11:893–897
5. Zhang JZ (2010) Biomedical applications of shape-controlled plasmonic nanostructures: a case study of hollow gold nanospheres for photothermal ablation therapy of cancer. J Phys Chem Lett 1:686–695
6. Kitur JK, Podolskiy VA, Noginov MA (2011) Stimulated emission of surface plasmon polaritons in a microcylinder cavity. Phys Rev Lett 106:183903
7. Nezhad MP, Simic A, Bondarenko O, Slutsky B, Mizrahi A, Feng L, Lomakin V, Fainman Y (2010) Room-temperature subwavelength metallo-dielectric lasers. Nature Photon 4:395–399
8. Oulton RF, Sorger VJ, Zentgraf T, Ma RM, Gladden C, Dai L, Bartal G, Zhang X (2009) Plasmon lasers at deep subwavelength scale. Nature 461:629–632
9. Lawandy NM (2004) Localized surface plasmon singularities in amplifying media. Appl Phys Lett 85:5040–5042
10. Bergman DJ, Stockman MI (2003) Surface plasmon amplification by stimulated emission of radiation: quantum generation of coherent surface plasmons in nanosystems. Phys Rev Lett 90:027402
11. Noginov MA, Zhu G, Belgrave AM, Bakker R, Shalaev VM, Narimanov EE, Stout S, Herz E, Suteewong T, Wiesner U (2009) Demonstration of a spaser-based nanolaser. Nature 460:1110–1112
12. Dice GD, Mujumdar S, Elezzabi AY (2005) Plasmonically enhanced diffusive and subdiffusive metal nanoparticle-dye random laser. Appl Phys Lett 86:131105
13. Meng XG, Fujita K, Murai S, Matoba T, Tanaka K (2011) Plasmonically controlled lasing resonance with metallic–dielectric core–shell nanoparticles. Nano Lett 11:1374–1378
14. De Luca A, Grzelczak MP, Pastoriza-Santos I, Liz-Marzan LM, La Deda M, Striccoli M, Strangi G (2011) Dispersed and encapsulated gain medium in plasmonic nanoparticles: a multipronged approach to mitigate optical losses. ACS Nano 5:5823–5829
15. Liu SY, Li JF, Zhou F, Gan L, Li ZY (2011) Efficient surface plasmon amplification from gain-assisted gold nanorods. Opt Lett 36:1296–1298
16. Fan XF, Shen ZX, Luk'yanchuk B (2010) Huge light scattering from active anisotropic spherical particles Opt Express 18:24868–24880
17. Gordon, JA, Ziolkowski RW (2007) The design and simulated performance of a coated nano-particle laser. Opt Express 15:2622–2653
18. Stockman MI (2010) The spaser as a nanoscale quantum generator and ultrafast amplifier. J Opt 12:1–13
19. Auguie B (2009) Optical properties of gold nanostructures. Ph.D. thesis, University of Exeter, United Kingdom
20. Jain PK, Huang WY, El-Sayed MA (2007) Noble metal nanoparticle pairs: effect of medium for enhanced nanosensing. Nano Lett 7:2080–2088
21. Bohren CF, Huffman DR (1983) Absorption and scattering of light by small particles. Wiley, New York
22. Myroshnychenko V, Rodriguez-Fernandez J, Pastoriza-Santos I, Funston AM, Novo C, Mulvaney P, Liz-Marzan LM, Garcia de Abajo FJ (2008) Modelling the optical response of gold nanoparticles. Chem Soc Rev 37:1792–1805
23. Hartland GV (2011) Optical studies of dynamics in noble metal nanostructures. Chem Rev 111:3858–3887
24. Noginov MA, Zhu G, Bahoura M, Adegoke J, Samll CE, Ritzo BA, Drachev VP, Shalaev VM (2006) Enhancement of surface plasmons in an Ag aggregate by optical gain in a dielectric medium. Opt Lett 31:3022–3024
25. Wuestner S, Pusch A, Tsakmakidis KL, Hamm JM, Hess O (2010) Overcoming losses with gain in a negative refractive index metamaterial. Phys Rev Lett 105:127401
26. Ni WH, Ambjornsson T, Apell SP, Chen HJ, Wang JF (2010) Observing plasmonic–molecular resonance coupling on single gold nanorods. Nano Lett 10:77–84
27. Cao M, Wang M, Gu N (2009) Optimized surface plasmon resonance sensitivity of gold nanoboxes for sensing applications. J Phys Chem C 113:1217–1221
28. Chern RL, Liu XX, Chang CC (2007) Particle plasmons of metal nanospheres: application of multiple scattering approach. Phys Rev E 76:016609
29. Noguez C (2007) Surface plasmons on metal nanoparticles: the influence of shape and physical environment. J Phys Chem C 111:3806–3819
30. Wang H, Tam F, Grady NK, Halas NJ (2005) Cu nanoshells: effects of interband transitions on the nanoparticle plasmon resonance. J Phys Chem B 109:18218–18222
31. Lakowicz JR (2006) Plasmonics in biology and plasmon-controlled fluorescence. Plasmonics 1:5–33
32. Schatz GC, Van Duyne RP (2002) Electromagnetic mechanism of surface-enhanced spectroscopy. In: Chalmers JM, Griffiths PR (ed) Handbook of vibrational spectroscopy. Wiley, New York, pp 759–774